Template Synthesis and Characterization of Layered Al− and Mg−Silsesquioxanes

L. Ukrainczyk,*,† R. A. Bellman,‡ and A. B. Anderson†

Departments of Agronomy and Materials Science and Engineering, Iowa State University, Ames, Iowa 50011

Received: September 24, 1996; In Final Form: November 20, 1996[⊗]

A series of new layered inorganic−organic nanocomposites, with organic functionalities directly bonded to an inorganic framework via the Si−C bond, were prepared by a template sol−gel synthesis. These layered Al− and Mg−silsesquioxanes were precipitated at room temperature by addition of aqueous base to an alcohol solution containing a mixture of $AlCl_3$ or $MgCl_2$ and a trialkoxysilane with a *n*-dodecyl, *n*-octyl, *n*-pentyl, 3-methacryloxypropyl, isobutyl, or phenyl functionality. The Si/Al and Si/Mg ratios of the reaction mixtures were 2:1 and 4:3, respectively, and were chosen to match the composition of clay mineral pyrophyllite (layered aluminosilicate) and talc (layered magnesiosilicate). X-ray diffraction and electron microscopy show that the products are crystalline with a layered structure. A comparison of basal spacings and length of the organic functionalities is consistent with a ∼10 Å inorganic layer and a bilayer arrangement of R groups for Al− silsesquioxanes and an interpenetrating arrangement of R groups for Mg−silsesquioxanes. FTIR and ^{13}C NMR spectra indicate that in the products the Si−C bond is intact and silanes are fully hydrolyzed, while the organic functionalities filling the interlayer space are in a solid-like environment. ^{29}Si NMR spectra reveal that silanes are not fully condensed and that the degree of condensation is higher in Mg−silsesquioxanes than Al−silsesquioxanes. Broad in-plane diffraction peaks and a variety of Al coordination states observed by ^{27}Al NMR are best explained by the defects in a clay-like inorganic framework caused by trifunctional Si. The most crystalline products were formed from long-chain alkyl−trialkoxysilanes with Al, while trialkoxysilanes with shorter R groups gave less well-organized structures. This dependence on chain length suggests that the formation of the layered structure is due to self-assembly of the hydrolyzed trialkoxysilanes into lamellar micelles. The micelles act as a template for the formation of a clay-like inorganic framework by condensation between the silanols and aqueous metal species attracted by the negatively charged surfactant layers. Although the thermal stability of R group limits high-temperature applications, these materials may find use as sorbents, environmental barriers, polymer fillers, catalytic supports, or chemical sensors.

Introduction

Incorporation of organic guest species by intercalation into expandable layered materials provides a unique opportunity to orient and manipulate intercalated species,[1,2] and to alter reactivity,[3] electronic,[4] and optical,[5] properties of both the guest and host. Furthermore, the ability to exfoliate layered materials such as smectites allows for preparation of small particles with large aspect ratio (thickness in a nanometer and diameter in a micrometer range) that can be used as fillers for polymers and coatings.[4b,6] The resultant polymer composites have been shown to have lower gas permeability and superior mechanical properties compared to traditional polymers and coatings.[6]

Among the many layered inorganic solids, smectites (swelling aluminosilicates or magnesiosilicates) occupy a special position owing to their adsorptive and ion exchange properties, thermal and chemical stability, swellability in polar solvents and ability to orient and form self-supported transparent films on drying.[2−4,5b,6] Two major limitations in the use of natural smectites for photochemical,[5b] environmental,[7] and filler[6] applications have been (i) the presence of impurities within clay mineral structure and on the surface and (ii) the inability to swell in nonpolar solvents and exfoliate in a polymer matrix. The impurities frequently cause discoloration and interfere with photofunctions of the guest or with its catalytic activity. Synthetic clay minerals, such as laponite, hectorite, and fluorohectorite, have been used frequently instead of natural clay minerals to avoid the impurities.[5b] In order to swell smectites in solvents of low polarity, to increase their affinity for such solvents[7,8] (e.g., for environmental applications), or to exfoliate them in a polymer matrix, inorganic interlayer cations need to be exchanged with organocations[6b,h] (typically quaternary alkylammonium ions) which have highly undesirable toxicological[9] properties limiting many applications. A possible alternative to use of organocations is to synthesize clay minerals with direct incorporation of polymers or other nontoxic organophilic functionalities in the interlayers.[10] However, synthesis methods for preparation of clay minerals with intercalated polymers, macrocycles, and organometallic complexes that have been reported so far require conditions similar to those for synthesis of conventional smectites: hydrothermal processing and carefully controlled reaction conditions for extended periods of time to crystallize the products.[10]

In the recent years it has been recognized that layered silicate structures, as well as many other crystalline inorganic materials, can be prepared under nonhydrothermal conditions by biomimetic template synthesis using self-organized assemblies of organic molecules.[11−18] In particular, synthesis routes using liquid crystal and surfactant micelles as templates have been subject of intense research.[11−35] For example, surfactants have been used for synthesis of mesoporous silicate and aluminosilicate molecular sieves and for preparation of organic−inorganic nanocomposites. A qualitative model of structural ordering and general surfactant template synthesis routes have been outlined by Monier et al.[15] and Huo et al.,[16] respectively. The ordering is thought to involve electrostatic interaction between inorganic monomers or oligomers and charged sur-

† Department of Agronomy.
‡ Department of Materials Science and Engineering.
* Corresponding author.
[⊗] Abstract published in *Advance ACS Abstracts,* January 1, 1997.

S1089-5647(96)02937-9 CCC: $14.00

factant headgroups. Because the ordering and growth of structures are observed below critical micelle concentration, as well as below the saturation with respect to the inorganic species, it has been proposed that micelle formation is promoted by the presence of inorganic species and that polymerization of inorganic species is promoted at the surfactant−water interface.[15,16]

The surfactants commonly used in the template synthesis have polar ends that do not become part of the inorganic framework. A possibility of the polar surfactant headgroup becoming a part of inorganic framework was suggested by Huo et al.[16] for layered structures prepared from a solution of phosphate surfactants and Zn hydroxide monomers and by Fukushima and Tani[36] for layered structures prepared from 3-methacryloyloxypropyltrimethoxysilane and Mg or Ni hydroxides. Headgroup and tail polymerization of surfactants has also been explored as a means to prepare polymeric surfactants (polysoaps) and polypeptide bilayers.[37]

In this study we investigated template synthesis of layered smectite-like materials using trialkoxy−organosilanes where polar ends are silanol groups that polymerize following the hydrolysis of alkoxy groups and become an integral part of the inorganic framework. Similar concepts have been explored in the synthesis of thin films grown on substrates by self-assembly of multilayers of organosilicon-[38] and zirconium[39] phosphate-derived materials. We describe sol−gel template synthesis of powders consisting of self-assembled layers of silanes with an organic functionality directly attached to silicon by Si−C bond and present structural characterization of the resultant layered organic/inorganic nanocomposites.

Materials and Methods

Synthesis. All the chemicals used were reagent grade and were used as received. *n*-Dodecyltriethoxysilane was obtained from Pfaltz & Bauer, and *n*-octyltriethoxysilane, *n*-pentyltriethoxysilane, phenyltrimethoxysilane, butyltrimethoxysilane, and 3-methacryloyloxypropyltrimethoxysilane were obtained from Gelest. For synthesis of Al−*n*-dodecylsilsesquioxane (AlnDS), Al−*n*-octylsilsesquioxane (AlnOS), Al−3-methacryloyloxypropylsilsesquioxane (AlMPS), Al−butylsilsesquioxane (AliBS), and Al−phenylsilsesquioxane (AlPhS), a volume of freshly prepared 0.4 M trialkoxysilane solution in a corresponding alcohol (ethanol or methanol) was mixed with an equal volume of 0.2 M $AlCl_3 \cdot 6H_2O$ (Fisher) in the alcohol. The alcohol solution was then titrated with 0.5 M aqueous NaOH (Fisher) while stirring until pH was 5.5. The addition of base to the alcohol solution of silane and $AlCl_3$ resulted in the formation of white gelatinous precipitate. The precipitate was aged for 24 h at room temperature and then washed repeatedly with distilled deionized water until no Cl^- could be detected in the filtrate. The white solid was air-dried at room temperature to give a white xerogel-like solid, which was gently ground and vacuum-desiccated for further analysis. For synthesis of Mg−*n*-dodecylsilsesquioxane (MgnDS), Mg−*n*-octylsilsesquioxane (MgnOS), Mg−3-methacryloyloxypropylsilsesquioxane (MgMPS), Mg−*I*-butylsilsesquioxane (MgiBS), and Mg−phenylsilsesquioxane (MgPhS), a volume of freshly prepared 0.27 M trialkoxysilane solution in a corresponding alcohol was mixed with an equal volume 0.2 M $MgCl_2 \cdot 6H_2O$ (Fisher) in alcohol. The alcohol solution was titrated slowly while stirring with 0.5 M NaOH until the suspension pH was 11.5. The white precipitate was aged, washed, and dried as described above for the Al samples.

Characterization. Elemental analysis was performed using Leco analyzer for C and H and microprobe for Si, Al, Mg, and Na. AlnDS sample was analyzed by Galbraith Laboratories, Inc. (Knoxville, TN), and was used for validating microprobe results. X-ray diffraction (XRD) patterns were recorded using Siemens D-5000 powder diffractometer with Cu Kα radiation (45/40 kV/mA), theta compensating slits, 0.02° step size, and 1°/min step. Thermal analysis was performed in air atmosphere using Seiko TG/DTA320 thermal analysis equipment, with a heating rate of 20 °C/min.

TABLE 1: Elemental Composition of Al− and Mg−Silsesquioxanes

	molar ratios		weight %	
	reaction mixture Si/M	product Si/M	C	H
AlnDS	2.00	2.14	53.3	9.9
AlnOS	2.00	2.15	45.7	8.2
AlnPS	2.00	0.71	24.8	6.2
AlMPS	2.00	1.25	33.0	5.2
AliBS	2.00	0.77	21.6	6.0
AlPhS	2.00	1.18	35.1	4.0
MgnDS	1.33	1.32	56.8	9.7
MgnOS	1.33	0.84	40.8	7.9
MgMPS	1.33	1.66	38.8	4.8
MgiBS	1.33	1.43	30.4	6.3
MgPhS	1.33	1.46	38.6	3.5

Solid state nuclear magnetic resonance (NMR) spectra for ^{27}Al were recorded by Spectral Data Services, Inc. (Champaign, IL), at 94 MHz with a single pulse, 0.3 s recycle time and using spinning rates of 8.4 kHz. Spectra were referenced relative to external 1 M $Al(H_2O)_6^{3+}$. ^{29}Si and ^{13}C NMR spectra were acquired at 59.6 and 75.5 MHz, respectively, using cross-polarization with magic angle spinning (CP/MAS) and spinning rates of 3.5 kHz on a Bruker MSL 300 spectrometer at the Iowa State University NMR Facility. Chemical shifts were referenced in ppm from external tetramethylsilane (0 ppm). Hexamethylsiloxane (−9.2 ppm) was used as a secondary reference for ^{29}Si. ^{13}C spectra were acquired with contact time of 3 ms and 4 s recycle time. ^{29}Si spectra were acquired with a 10 s recycle time.

Transmission electron microscopy (TEM) was performed on the samples deposited as dispersions in ethanol on a copper grid with a holey carbon film using a Jeol 1200EX microscope operating at 120 keV and a Phillips CM-30 operating at 300 keV. Scanning electron microscopy (SEM) was performed on the air-dried powder samples glued with silver paint on brass pegs using a Jeol JSM-35 microscope. Fourier transform infrared (FTIR) spectra were obtained with Digilab Biorad FTS-40 spectrometer using diffuse reflectance (DRIFT) accessory. Single-beam spectra of samples in KBr matrix were obtained by averaging 64 scans at 4 cm^{-1} resolution and were referenced against KBr background.

Results

Synthesis. The Si/Al molar ratios of the reaction mixtures and products and the carbon content of the products are presented in Table 1. The Si/C molar ratios of the products are identical to those expected for each of the silanes, suggesting that the Si−C bond remained intact during synthesis, alcohol has been removed from the material, and silanes remaining in the solid are completely hydrolyzed. For the two long-chain Al−alkylsilsesquioxanes, AlnDS and AlnOS, the Si/Al molar ratios are close to those of the reaction mixture, and the composition is close to that of the clay mineral-like structure $(RSi)_4Al_2O_8(OH)_2$. On the contrary, other Al products are deficient in Si and C, indicating silane was lost during washing. Increasing pH (>5.5 for Al products, >11.5 for Mg products), varying water/alcohol ratio (by using 0.05 M NaOH instead of

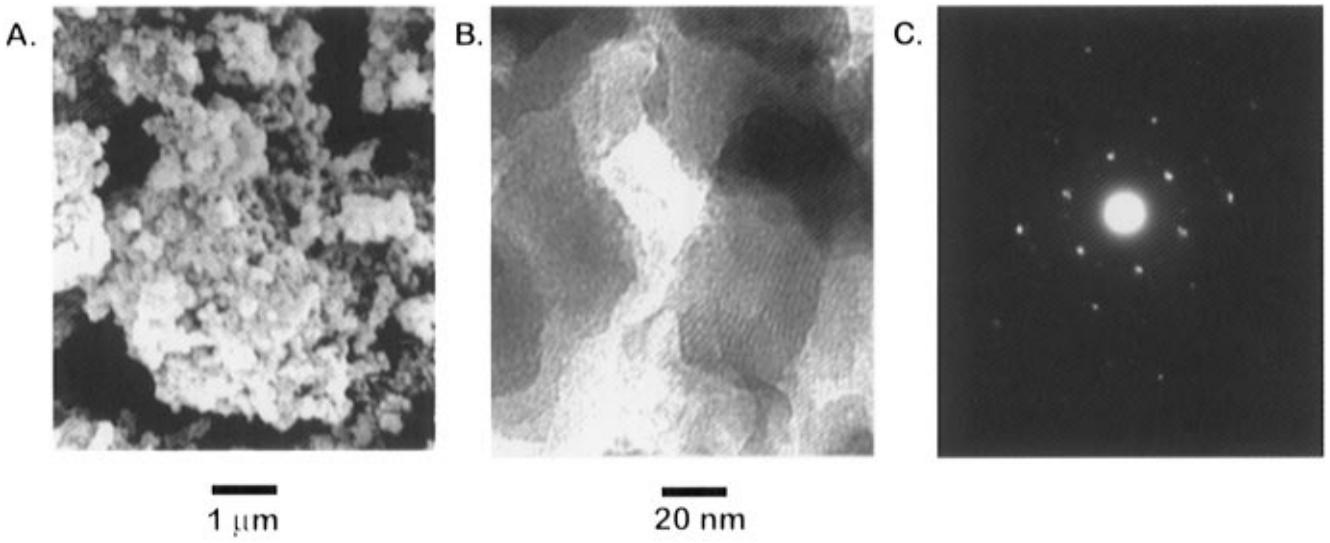

Figure 1. (A) SEM micrograph of AlnDS. (B) TEM micrograph showing layered morphology and (C) SADP of AlnDS in the direction perpendicular to the layers.

0.5 M NaOH), and prolonging the aging of the synthesis mixture had no effect on the stoichiometry of the products. Lowering the pH of the Al−silsesquioxane synthesis mixture below 5 usually resulted in leaching and loss of Al during washing of the products. While synthesis of Al−silsesquioxanes was reproducible and gave identical products over a wide range of conditions (for example, stoichiometry and XRD patterns were insensitive to slow or fast addition of base and variable water/alcohol ratios), synthesis of Mg−silsesquioxanes required slow, carefully controlled addition of base. If the pH of Mg−silsesquioxane synthesis mixture was raised too quickly, greasy, oily, sticky white, or transparent products were obtained. It has been reported previously that the hydrolysis of trialkoxy−organosilanes is more rapid at pH 3−4 than at higher pH.[40] Since base catalyzed hydrolysis of silanes requires inversion of the Si tetrahedra,[41] the presence of the bulky alkyl substituent on Si is likely to make hydrolysis more difficult at high pH where Mg−silsesquioxanes were precipitated. Separation of oily products from alkyl−trialkoxy silanes has been reported previously in aqueous solutions of alkali metal aluminates and attributed to formation of insoluble cyclic siloxane oligomers.[42,43] Thus, the sticky oily products observed in this study are likely similar siloxane oligomers.

The washed and air-dried Al− and Mg−silsesquioxanes could not be dispersed in water (they float) but could be dispersed in alcohols (except methanol) and nonpolar solvents. The affinity of the silsesquioxanes toward organic solvents increased with longer and less polar R groups. Silsesquioxanes are known to create hydrophobic surface that have water contact angles greater than 90° and consequently are not expected to adsorb water.[44,45]

Electron Microscopy. The SEM and TEM micrographs of the AlnDS (Figure 1A,B) reveal the platelike morphology of the product with an average particle size of 100 nm. Moire fringing was observed in TEM where platelets were stacked and the beam was perpendicular to the platelets (Figure 1B), indicating that the particles are crystalline. The selected area diffraction pattern (SADP) obtained from AlnDS (Figure 1C), shows hexagonal symmetry in the plane of the platelet, with spacings of 4.2, 2.4, and 1.5 Å. The SADP patterns were difficult to observe and could only be seen for areas such as that shown in Figure 1B, where several platelets were stacked. The difficulty in obtaining the patterns may be due to both the turbostratic arrangement of the silsesquioxane platelets[46] or to the beam damage of the sample,[47] a common problem in imaging clay minerals by electron microscopy.

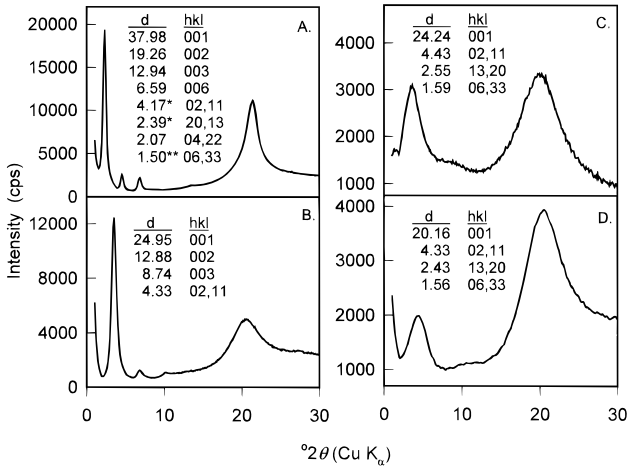

Figure 2. Powder XRD patterns of Al− and Mg−silsesquioxanes: (A) AlnDS (*reflections observed in both XRD and electron diffraction pattern; **reflections observed in the electron diffraction pattern only), (B) AlnOS, (C) MgnDS, and (D) MgnOS.

XRD. The powder XRD patterns of the Al− and Mg−silsesquioxanes (Figure 2A,B) resemble those of smectites, with one or more rational orders of the largest *d* spacing (basal reflection) and several broad higher angle (in-plane) reflections.[48] The long-chain Al−silsesquioxanes exhibit four or more rational orders of the basal peak, with layer spacings of up to 38 Å. The absence of reflections at noninteger orders of the basal spacing is indicative of a lamellar structure.[49] The XRD patterns of the corresponding Mg structures (Figure 2C,D), as well as those of other silsesquioxanes (Figure 3) exhibit much broader basal peaks, implying these structures are less well ordered. Most patterns have only two or three in-plane peaks. For AlnDS, these in-plane peaks correspond to the spacings observed in the SADP. The broad in-plane peaks and lack of (*hkl*) reflections, common in layered materials, is indicative of either the disordered inorganic framework or/and the turbostratic arrangement of the plates.[48,49] An in-plane reflection at 59.2° 2θ was present only in Mg−containing structures. This peak is of the same spacing as the (060) reflection observed in smectites.[48]

The plot of the R group length vs basal spacing, presented in Figure 4A, shows that the basal spacing is proportional to

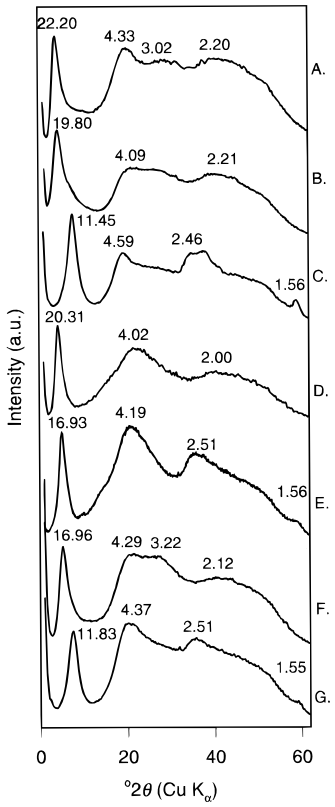

Figure 3. Powder XRD patterns of Al− and Mg−silsesquioxanes: (A) AlnPS , (B) AliBS, (C) MgiBS, (D) AlMPS, (E) MgMPS, (F) AlPhS, and (G) MgPhS.

the length of the organic functionality and that Mg−silsesquioxanes consistently have smaller layer spacing than Al−silsesquioxanes. The basal spacing for the Al−silsesquioxanes is approximately equivalent to the sum of the twice the length of the extended R group plus the van der Waals thickness of a 2:1 clay layer (9.6 Å), suggesting that in the Al−silsesquioxanes R groups are organized into lamellar bilayers filling the "interlayer" space between Al/Si inorganic framework. The deviation of the basal spacings from the straight line representing 2R + 9.6 Å in Figure 4A is likely due to variations in the conformation of R groups in the interlayers (e.g., not fully extended or partially interpenetrating). The exact conformation of R groups cannot be determined from experimental data presented here. The basal spacing of Mg−silsesquioxanes is approximately equal to the length of the R group plus 9.6 Å, indicating different ordering of R groups. Although the arrangement of R groups cannot be conclusively established from the data presented here, the basal spacing of Mg−silsesquioxanes is consistent with an alternating surfactant monolayers[50,51] filling the interlayer space (Figure 4C). The relatively large spacing of MgMPS is also consistent with the proposed arrangement, because the branched structure of 3-methacryloyloxypropyl group should allow only partial interpenetration between the two opposing monolayers. The difference in the arrangement of organic chains in the interlayers could be due to the different micelle structures of the silane precursors in solution or to the different hydrolysis rates and mechanisms, as well as different condensation rates when preparing Al− and Mg−silsesquioxanes: Mg structures form gels at pH > 10, while Al structures gel at pH < 4.

The degree of ordering in the layered silsesquioxanes was investigated by comparing the breadth of the XRD basal peak to the R group length. The raw XRD spectra were corrected for Lorentz polarization factor for random powders,[52] and for the changes in the irradiated sample volume produced by the theta compensating slits.[53] No corrections for instrument broadening were performed since the basal peaks were fairly broad.[54] The FWHM of the first three orders of the basal peaks in AlnDS and AlnOS increased by about 1/cos θ.[55] Because this increase in fwhm is consistent with the Scherrer equation, the peak broadening was attributed to the tactoid size (thickness of a region of coherently diffracting platelets). The average number of coherently scattering layers is plotted against the R group length for the Al− and Mg− silsesquioxanes in Figure 4B. It can be seen that the ordering of the Al−silsesquioxanes increases with longer R groups, suggesting that ordering into a lamellar structure is dominated by surfactant interactions. In contrast, the ordering of Mg−silsesquioxanes decreases with increasing R group length, suggesting that surfactant interactions are less dominant in the ordering of the Mg−silsesquioxanes.

Assuming a smectite-like structure, the in-plane lattice parameter, *b*, of silsesquioxanes was calculated from nonbasal reflections (Figure 4A). The *b*-dimension is consistently smaller for Al−silsesquioxanes (average *b* is 8.47 ± 0.29 Å) compared to Mg−silsesquioxanes (average *b* is 9.40 ± 0.08 Å). These values are close[56] to the ideal *b* dimensions of a dioctahedral gibbsite-like ($Al(OH)_3$) sheet (8.64 Å) and of a trioctahedral brucite-like ($Mg(OH)_2$) sheet (9.36 Å), which supports the proposed structure as well as the assumption that the XRD reflections are due to both inorganic and organic structural components.

FTIR. The FTIR spectra of the Al− and Mg−silsesquioxanes show that the R groups are unreacted and the direct Si−C bond is retained.[57] Comparison of the FTIR spectra of AlnDS and MgnDS (Figure 5) reveals several differences between the Al and Mg structures. Bands corresponding to the *n*-dodecyl group are much sharper in the spectrum AlnDS compared to MgnDS, consistent with higher crystallinity of the Al−silsesquioxane. The width of Si−OH band at 3344 cm^{-1} in the spectrum of AlnDS is likely due to a Si−OH groups forming solidlike hydrogen bonds.[58] In addition, Figure 5 shows that the methylene rocking vibration, ρCH_2, of *n*-dodecyl group is split into a doublet. This splitting, which occurs in the spectra of solid *n*-alkanes, is indicative of a rigid environment of the organic functionalities.[59] The splitting of the methylene rocking vibration is observed in all Al− and Mg−*n*-alkylsilsesquioxanes synthesized.

^{13}C Solid State NMR. The ^{13}C CP/MAS spectrum of the AlnDS shows four peaks at 37.0 (shoulder), 32.7, 24.2, and 14.4 ppm (Figure 6A). The ^{13}C spectra obtained without cross-polarization showed no additional resonances,[60] indicating there are no highly mobile, liquidlike methylene or methyl groups.[61] Assignments shown in Figure 6A are based on previous ^{13}C NMR studies of alkylsilanes horizontally polymerized on silica surface.[62] Broad, unresolved methylene groups and spinning sidebands show that the alkyl chains of AlnDS are in a rigid, solidlike environment.[62,63] The ^{13}C CP/MAS spectra of other Mg− and Al−silsesquioxanes exhibit similar features.

^{29}Si Solid State NMR. ^{29}Si CP/MAS NMR spectra of AlnDS, MgnDS, AlPhS, and MgPhS are shown in Figure 7. All the spectra have three peaks in the chemical shift range of the trifunctional silicon (T) and no resonance in the silicate region, confirming that Si−C bond remained intact during synthesis.[64] The T^n notation used to describe silicon sites for silsesquioxanes is similar to the Q^n notation used for silicates where superscript refers to the number of bonds to other silicon atom through an oxygen bridge: T^0 stands for a monomer ($Si(R)(OR')_3$, where R = organic moiety bonded to Si by Si−C bond; R′ = H, or alkyl group depending on the degree of hydrolysis), and T^1, T^2, and T^3 refer to silicons with one

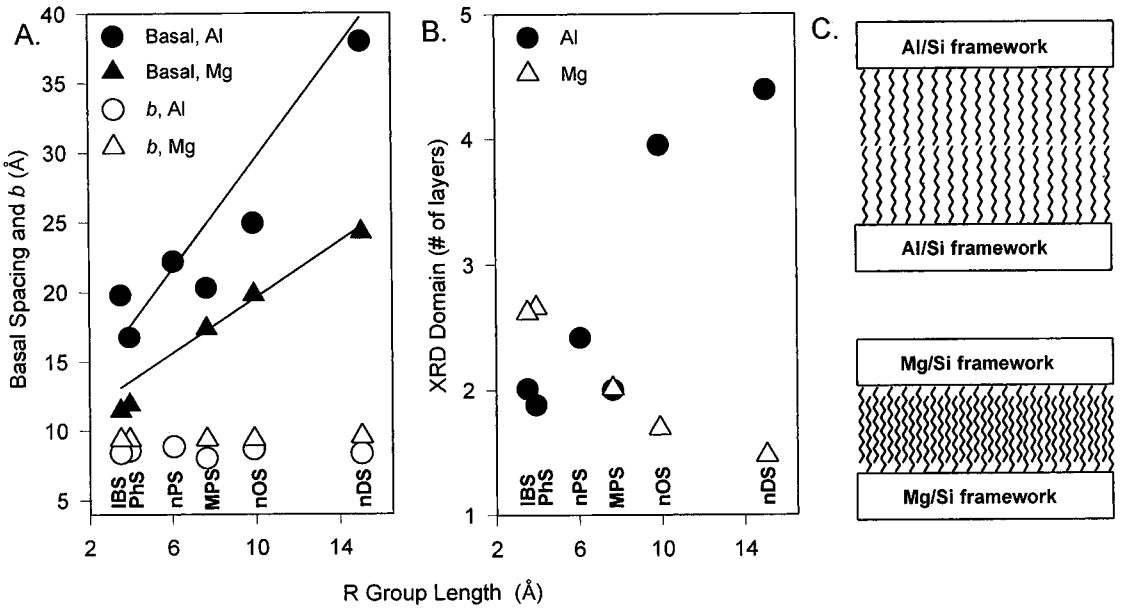

Figure 4. (A) Plot of basal spacing and *b* dimension vs the fully extended R group length. Lines represent ideal R + 9.6 Å and 2R + 9.6 Å plots. (B) Plot of tactoid size vs R group length. (C) Proposed arrangement of ligand chains in Al− and Mg−silsesquioxanes.

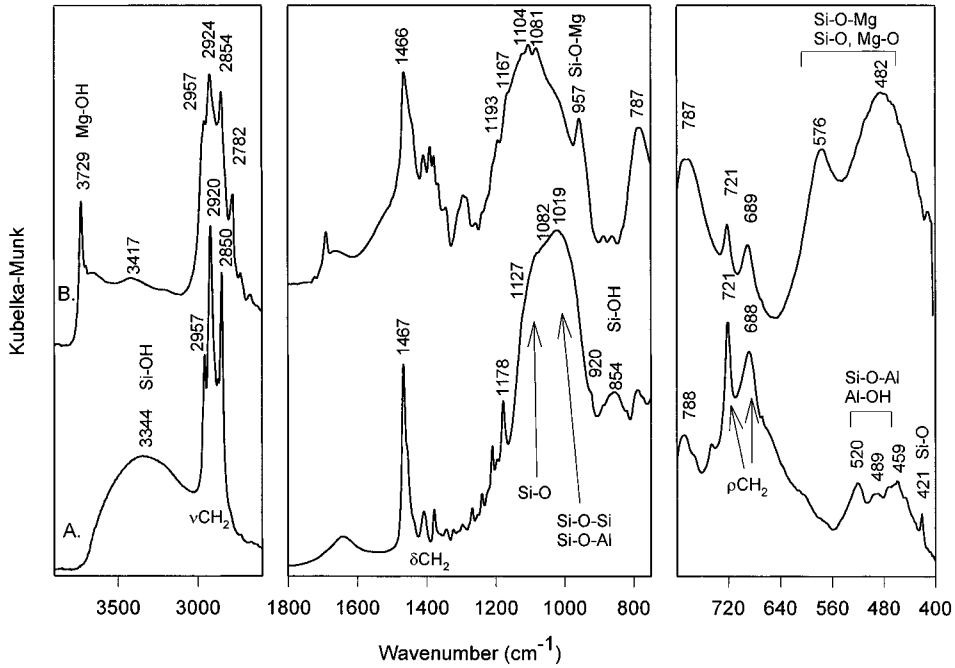

Figure 5. DRIFT spectra of (A) AlnDS and (B) MgnDS.

$(Si(R)(OR')_2OSi)$, two $(Si(R)(OR')(OSi)_2)$, and three $(Si(R)(OSi)_3)$ siloxane bonds, respectively.[40,64] For solid organosilicon polymers or organosilanes grafted to silica surface, the ^{29}Si chemical shifts of T^3 silicon are −65 to −70 ppm (R = alkyl)[64] and −75 to −80 ppm (R = phenyl),[64] while T^2 and T^1 silicon are shifted downfield from T^3 by approximately 10 and 20 ppm, respectively.[60,64,65] The ^{29}Si chemical shifts of the three peaks in all the spectra shown in Figure 6 are clearly in the chemical shift range of T^1, T^2, and T^3 silicon. Because all of the silsesquioxane products were extensively washed with distilled water, it is unlikely that any alkoxy groups remained in the solid. In addition, no residual alkoxy groups could be detected in the FTIR and ^{13}C NMR spectra. Thus, the T^n silicons in Al− and Mg−silsesquioxanes are bonded either to a hydroxyl group or to other Si, Al, or Mg atoms through an oxygen bridge.

Several features are observed when comparing the ^{29}Si spectra of Al−silsesquioxanes to those of corresponding Mg−silsesquioxanes. It can be seen that for MgnDS and MgPhS the T^3 peak is more intense compared to AlnDS and AlPhS, indicating the higher degree of condensation for Mg−silsesquioxanes compared to Al−silsesquioxanes. In Al−silsesquioxanes the T^3 peak is shifted downfield relative to the Mg−silsesquioxanes by 3.6 ppm (nDS) and 3.7 (PhS) ppm, which is consistent with the presence of Si−O−Al linkages. For example, the ^{29}Si shift in clay minerals is 4 ± 2 ppm downfield when going from Si in the tetrahedral sheet that has no Al isomorphous substitution ($Q^3(0Al)$) to one tetrahedral Al substituted into the second coordination sphere of Si ($Q^3(1Al)$).[66] However, the ^{29}Si resonance also shifts in clay minerals with $Q^3(0Al)$ units by 1−3 ppm downfield for dioctahedral clay minerals with mainly Al in octahedral sheet compared to trioctahedral clay minerals with mainly Mg in octahedral sheet.[64] Assuming that silsesquioxanes have an inorganic framework similar to the clay minerals, it follows that the T^3 shifts observed

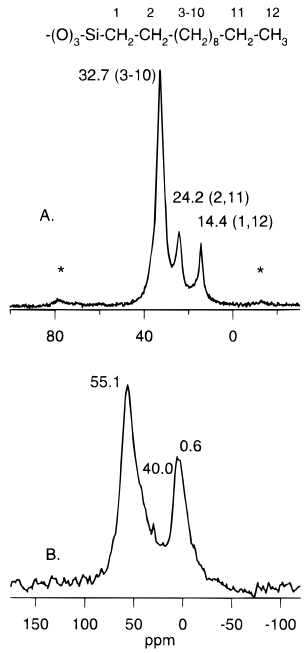

Figure 6. (A) ^{13}C CP/MAS NMR spectrum (* denotes spinning sidebands) and (B) ^{27}Al MAS NMR spectrum of AlnDS.

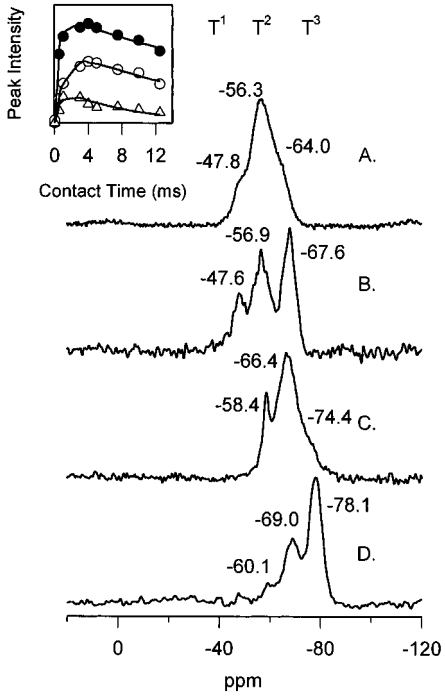

Figure 7. ^{29}Si CP/MAS spectra of (A) AlnDS with a plot of T^1, T^2 and T^3 peak intensities vs contact time, (B) MgnDS, (C) AlPhS, and (D) MgPhS. All four spectra were acquired with contact time of 4 ms and 10 s recycle time.

for Al−silsesquioxanes could be due either to tetrahedral substitution of Al for Si or to the Al in "octahedral" sheet sharing an oxygen with the Si tetrahedron. Interestingly, the other two ^{29}Si peaks of AlnDS are not shifted downfield relative to the corresponding peaks in MgnDS, which makes it highly unlikely that there is Al substitution in the "tetrahedral" sheet of AlnDS.[66] On the contrary, T^2 and T^1 peaks of AlPhS are shifted by 2.6 and 1.7 ppm relative to MgPhS. This observation along with the low Si/Al ratio of AlPhS (Table 1) suggests that Al may be in the tetrahedral sheet of AlPhS.

The high degree of structural organization for AlnDS and AlnOS, where chain length is sufficient to allow for significant van der Waals interaction,[67] as well as the lack of ordering for products with shorter R groups strongly supports the hypothesis that ordering in Al−silsesquioxanes is mainly due to hydrophobic surfactant chain interaction and formation of lyotropic liquid crystals, rather than to grafting of silanes to the preformed octahedral Al hydroxy sheets. The organization of Mg−silsesquioxanes is likely to proceed in a different manner because at high pH silanol groups will be condensing more rapidly to form Si−O−Si and Si−O−Mg bonds.[41,68] This will effectively increase headgroup area of the silanol surfactant and may result in the interpenetrated chain structure suggested by XRD results.[50,67] However, other arrangements of the R groups cannot be ruled out.

Because the peak intensities in the CP/MAS technique depend on $T_{1\rho H}$ and on the efficiency of cross-polarization, the relative intensities in the spectra must be corrected for the differences in magnetization rates by performing variable contact time studies.[69] The proportion of Si contributing to each peak in AlnDS spectra was determined by normalizing the peak areas in Figure 7A to cross-polarization efficiencies of each of the three peaks calculated by fitting the peak intensity vs contact time data in Figure 7A to eq 1[69]

$$I = \frac{I_0}{1 - k_1/k_2}[\exp(-k_1 t) - \exp(-k_2 t)] \qquad (1)$$

where k_1 is the relaxation rate in rotating frame ($1/T_{1\rho H}$), k_2 is the rate of cross-polarization ($1/T_{SiH}$), t is contact time, I is peak intensity, I_0 is the intensity under conditions of full cross-polarization and no relaxation, and I/I_0 is the cross-polarization efficiency. The T^1 peak at −46.6 ppm gives maximum magnetization at very short cross-polarization times (1 ms), due to a greater number of neighboring hydrogens than the other two peaks. These peaks correspond to a more condensed Si and show a maximum cross-polarization efficiency at contact times between 3 and 5 ms. Using corrected peak intensities, the relative proportions of the T^1, T^2, and T^3 Si in AlnDS are calculated to be 10, 66, and 24%, respectively.

^{27}Al Solid State NMR. The ^{27}Al MAS NMR spectrum of AlnDS (Figure 6B) shows the presence of 4-coordinate (55.1 ppm), 5-coordinate (40.0 ppm), and 6-coordinate (0.6 ppm) Al. The ratio of peak areas, obtained by deconvolution and curve fitting of the spectra, is $Al^{IV}/Al^{V}/Al^{VI} = 41:29:30$. As indicated in the above analysis of ^{29}Si spectra, the 4-coordinate Al may be substituting for Si in the "tetrahedral" layer. However, both 4- and 5-coordinate Al may be due to Al in the "octahedral" layer which is lacking oxygens that it would normally share with the silicon tetrahedra. Using elemental analysis data in Table 1 and semiquantitative analysis of ^{27}Al and ^{29}Si NMR spectra for AlnDS, it can be seen that per every T^3 Si there is approximately 1 Al^{IV} and 0.5 Al^{V}. A side view of the AlnDS structure (Figure 8B) shows how the different Al coordinations may be accommodated within the distorted" octahedral sheet. (A side view of a clay mineral[56] is shown for comparison in Figure 8A.) The proposed structure (Figure 8B) may also account for the fact that in AlnDS T^2 and T^1 Si resonances are not shifted relative to those of MgnDS: only T^3 Si is bonded to Al via Si−O−Al bond.

Thermal Analysis. Thermal stability of silsesquioxanes was investigated by DTA/TGA. DTA curves of the silsesquioxanes display up to four exothermic peaks (Table 2) that can be assigned, based on the observed weight loss, to pyrolysis of the organic group (exotherms I−II), dehydroxylation and collapse of the layered structure (III), and recrystallization of the pyrolysis product to oxides and carbides (IV). The R group

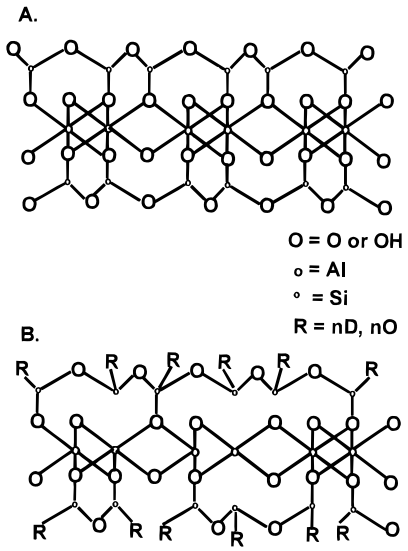

Figure 8. Side view of (A) a 2:1 aluminosilicate clay layer and (B) a schematic presentation of inorganic framework of AlnDS showing 4-, 5-, and 6-coordinate Al.

TABLE 2: Thermal Analysis of Al− and Mg−Silsesquioxanes

	DTA exotherms (°C) (weight remaining)				TG (%) weight[a]
	I	II	III	IV	remaining
AlnDS	251 (80.4)[b]	405 (47.5)	495 (39.1)		31.5
AlnOS	259 (83.7)	398 (60.6)	439 (57.2)		45.7
AlnPS	302 (75.3)	440 (57.6)	500 (55.8)	993 (52.3)	52.3
AlMPS	408 (69.4)		464 (59.6)	1017 (40.9)	40.9
AlIBS	290 (72.0)	430 (56.8)	464 (55.9)	1002 (52.4)	52.4
AlPhs	240 (61.8)		489 (50.7)	1010 (49.6)	49.6
MgnDS	281 (76.0)	348 (65.3)	532 (29.8)		28.0
MgnOS	290 (86.3)	412 (56.0)	471 (47.5)	873 (43.6)	43.5
MgMPS	398 (63.4)	480 (47.5)	540 (43.0)	915 (40.7)	40.7
MgIBs	246 (87.8)	470 (59.5)	563 (53.1)		51.0
MgPhS	418 (70.2)		630 (48.1)	918 (45.9)	45.9

[a] After heating in air to 1150 °C at 20 °C/min. [b] Values in parentheses are in %.

pyrolysis temperature decreases with increasing alkyl chain length except for AlMPS and MgMPS in which the methacrylate R groups cross-link at 200 °C to form a more stable polymeric species. The R group pyrolysis temperatures are lower for the Si-deficient samples than for those that have a Si/M ratio close to that of reaction mixture and for the Al−silsesquioxanes compared to the corresponding Mg products, possibly due to the acidity of the Al. The greater thermal stability of the Mg−silsesquioxanes over Al−silsesquioxanes parallels that of trioctahedral clay minerals over dioctahedral clay minerals.[70] This greater stability toward dehydroxylation is believed to arise for the higher occupancy of the octahedral sheet, producing a more uniform charge distribution about the structural hydroxyl.[70]

The crystallized material remaining after heating to 1150 °C was examined by XRD. Mg−silsesquioxanes recrystallized into enstatite, forsterite, and cristobalite at approximately 800 °C. Interestingly, these products are also observed for recrystallization of talc,[71] a 2:1 trioctahedral clay mineral ($Mg_3Si_4O_{10}(OH)_2$). Similarly, Al−silsesquioxanes recrystallize at 1000 °C into mullite, which is also formed by the recrystallization of pyrophyllite ($Al_2Si_4O_{10}(OH)_2$).[71] In addition, recrystallization of Al−silsesquioxanes yielded silicon carbide, whereas no silicon carbide was observed on recrystallization of Mg−silsesquioxanes. Weight losses observed are consistent with the conversion of the measured compositions to these oxides and carbides.

Discussion

The narrow, high-intensity basal peaks in the XRD patterns of AlnDS and AlnOS (Figure 2A,B), as well as platelike morphology evident in electron micrographs (Figure 1A,B), indicate that acid-catalyzed hydrolysis and condensation of long-chain alkyltrialkoxysilanes results in the formation of layered, ordered materials. The fact that other trialkoxysilanes with shorter R groups give less well-organized structures under the same hydrolysis and condensation conditions suggests that the ordering into layers is driven primarily by surfactant interactions (Figure 4B). Under acidic conditions, rate of hydrolysis of silanes is fast relative to the rate of condensation.[41] While hydrolysis of trialkoxysilanes results in surfactant-like molecules with hydrophobic organic groups and hydrophilic silanol groups,[42] condensation of silanols effectively leads to surfactants with large headgroups and multiple chains. Such surfactants are known to form stable lamellar phases.[50,67,72] The partially condensed silanol groups in a lamellar surfactant phase are acidic, resulting in a negative layer charge of the surfactant phase. This negative charge attracts positively charged aqueous Al species which condense to form an inorganic framework.[16]

The exceptional ordering observed with longer-chain Al−alkylsilsesquioxanes is not observed in the corresponding Mg−alkylsilsesquioxanes (Figure 4B). The decrease in the *d* spacings for Mg−silsesquioxane structures is consistent with a layered structure with interpenetrating organic groups in the interlayers (Figure 4C), similar to surfactant H-phases[51] and alternating surfactant monolayers observed for water gel phases.[50] The ^{29}Si NMR data indicate higher degree of condensation of silanes, which is characteristic of base-catalyzed hydrolysis. Under basic pH conditions where the Mg−silsesquioxanes are formed, hydrolysis of silanes requires formation a of 5-coordinate intermediate and an inversion of the center (S_N2 mechanism).[41] The rate of hydrolysis is slow relative to the rate of condensation. Furthermore, basic pH favors formation of Si−O−Mg and Mg−O−Mg bonds,[68] which would space out the R groups of silanes. This may lead to decreased surfactant interactions among species in the same layer and penetration of the organic functionalities from another layer.

Unless base addition was slow, lamellar surfactant structures were not formed from trialkoxysilane/Mg mixtures and condensation resulted in oily products, most likely insoluble cage oligomers.[42,43] It may be inferred that when the rate of hydrolysis is fast relative to the rate of condensation, surfactant ordering into liquid crystals is favored. Conversely, strongly basic conditions under which condensation is rapid favor formation of cyclic siloxane cages over surfactant ordering, because monomeric surfactants are rapidly condensed before micelle formation can occur.

The striking similarity of both Al− and Mg−silsesquioxanes to surfactant−water gel phases[50] further supports the argument that these products result form self-assembly of surfactant-like R groups. Surfactants with large headgroups and multiple chains are known to form stable lamellar liquid crystals[67,72] and lamellar surfactant-and-water gel phases with a solidlike arrangement of hydrophobic chains.[50] Gel phases are observed, for example, in dialkyl lipids such as lecithin which form gels with a bilayer arrangement of chains,[73] monoglycerides which form bilayers with tilted chains,[50] and potassium soaps which form gels with interpenetrating chains.[74] Similar to gel phases, the Al− and Mg−silsesquioxanes are lamellar, with a basal spacing independent of the silane and water concentrations.[74,75] The splitting of methylene rock[73] observed in the FTIR spectrum (Figure 5) and the broad unresolved CH_2 resonances observed in the ^{13}C CP/MAS NMR spectrum (Figure 6A) confirm that

the hydrophobic R groups are in a solidlike arrangement. Furthermore, the 4.2 Å peak observed by XRD (Figure 2A,B), and the hexagonal SADP pattern (Figure 1C) are typically observed in gel phases where they are attributed to crystalline ordering of the paraffin chains into a hexagonal array.[73−75] In the formation of the Al− and Mg−silsesquioxanes, this crystalline ordering of the organic functionalities forms a template for the condensation of the silanol headgroups with aqueous metal species to form a claylike structure.

An alternative mechanism to self-assembly of Al− and Mg−silsesquioxanes by lamellar surfactant micelle formation would be the formation of gibbsite- and brucite-like dioctahedral and trioctahedral sheets to which silanol groups would be grafted to give the observed layered structure. Because this mechanism implies that the ordering is imposed by inorganic layers, it should be independent of surfactant properties of the silane R groups. Therefore, it can be ruled out for Al−silsesquioxanes, where a strong dependence is observed between the degree of crystallinity and surfactant properties of the R group (Figure 4B). However, in the case of Mg−silsesquioxanes the best surfactant does not give the most crystalline structure, probably because it is the bulkiest and sterically hinders hydrolysis. Thus, the ordering into layers of Mg−silsesquioxanes may be partly driven by the formation of trioctahedral brucite-like sheets.

Evidence of incorporation of Al and Mg into a structured inorganic framework comes from the similarity of the *b* lattice parameters determined by XRD to those of the ideal dioctahedral and trioctahedral sheets (Figure 4A). However, ^{29}Si NMR shows broad peaks (Figure 7), consistent with a variety of bond distances and angles in the inorganic layer, and ^{27}Al NMR (Figure 6b) shows that Al exists in 4-, 5-, and 6-fold coordination. This is not surprising since each Si has only three oxygens, thus formation of a claylike structure will require introduction of defects in the Al coordination sphere. Additional NMR and diffraction studies are underway to gain further insight into the structure of the inorganic layer.

Conclusions

Hydrolysis and condensation of trialkoxysilanes in a water/alcohol mixture containing $AlCl_3$ or $MgCl_2$ results in the rapid formation of layered claylike inorganic/organic nanocomposites (Al− and Mg−silsesquioxanes) that have organic functionalities directly bonded to the inorganic framework via Si−C bond. The self-assembly of the structure into layers is driven by the formation of lamellar micelles from silane triols. This lamellar structure acts a template for formation of a claylike inorganic framework by condensation between the silanols and aqueous metals species attracted by the negatively charged surfactant layers. The XRD data are consistent with a ∼10 Å inorganic layer and a bilayer chain arrangement for Al−silsesquioxanes and an interpenetrating arrangement of R groups for Mg−silsesquioxanes.

The degree of ordering is highest for AlnDS and AlnOS, which are prepared from silanes with long-chain alkyl groups at low pH where rate of hydrolysis is fast relative to the rate of condensation. However, the same silanes gave poorly ordered layered structures when precipitated with Mg at high pH. In this regime, the rate of condensation is fast relative to the rate of hydrolysis, and hydrolysis is hindered by bulky substituents on Si because it requires an inversion of the center.

The Al− and Mg−silsesquioxanes show strong affinity toward organic solvents, and can be dispersed in organic solvents to make oriented films. The hydrophobicity and other properties of the silsesquioxanes may be altered by the choice of the organic functionality of the trialkoxysilane. Although the thermal stability of R group limits high-temperature applications, these materials may find use as sorbants, environmental barriers, polymer fillers, catalytic supports, or chemical sensors.

Acknowledgment. This research was supported by Iowa Agricultural Experiment Station (IAHEES Journal Paper No. J-17188).

References and Notes

(1) (a) Whittingham, M. S.; Jacobson, A. J. *Intercalation Chemistry*; Academic Press: New York, 1982. (b) *Molecular Dynamics in Restricted Geometries*; Klafter, J., Drake, J. M., Eds.; Wiley-Interscience: New York, 1989.

(2) Barrer, R. M. *Zeolites and Clay Minerals as Sorbents and Molecular Sieves*; Academic Press: London, 1978.

(3) (a) Jordan, J. W. *J. Phys. Colloid Chem.* **1950**, *54*, 294. (b) Pinnavaia, T. J. *Science* **1983**, *220*, 4595. (c) Ukrainczyk, L.; Chibwe, M.; Pinnavaia, T. J.; Boyd, S. A. *Environ. Sci. Technol.* **1995**, *29*, 439. (d) Chibwe, M.; Ukrainczyk, L.; Boyd, S. A.; Pinnavaia, T. J. *J. Mol. Catal.* **1996**, *113*, 249.

(4) (a) Clearfield, A. *Chem. Rev.* **1988**, *88*, 125. (b) Mehrotra, V.; Giannelis, E. P. *Mater. Res. Soc. Symp. Proc.* **1990**, *171*, 39. (c) Ruiz-Hitzky, E. *Adv. Mater.* **1993**, *5*, 334. (d) Mitzl, D. B.; Feild, C. A.; Harrison , W. T. A.; Guloy, A. M. *Science* **1994**, *369*, 467.

(5) (a) Jones, W. In *Photochemistry of Organized and Constrained Media*; Ramamurthy, V., Ed.; VCH Publishers: New York, 1991; Chapter 9. (b) Ogawa, M.; Kuroda, K. *Chem. Rev.* **1995**, *95*, 399.

(6) (a) Ferrigno, T. H. In *Handbook of Fillers and Reinforcements for Plastics*; Katz, H. S., Milewski, J. V., Eds.; Van Nostrand Reinhold: New York, 1978; Chapter 2. (b) Okada, A.; Kawasumi, A.; Kojima, Y.; Kurauchi, T.; Kamigaito, O. *Mater. Res. Soc. Symp. Proc.* **1990**, *171*, 45. (c) Chang, S.-H.; Ryan, M. E.; Gupta, R. K.; Swiatkiewicz, B. *Colloids. Surf.* **1991**, *59*, 59. (d) Sonobe, N.; Kyotani, T.; Tomita, A. *Carbon* **1991**, *29*, 61. (e) Giannelis, E. P. *JOM* **1992**, *44*, 28. (f) Messersmith, P. B.; Giannelis, E. P. *Chem. Mater.* **1993**, *5*, 1064. (g) Ogawa, M.; Takahashi, M.; Kuroda, K. *Chem. Mater.* **1994**, *6*, 715. (h) Pinnavaia, T. J.; Lan, T.; Kaviratna, P. D.; Wang, M. S. *Mater. Res. Soc. Symp. Proc.* **1994**, *346*, 81.

(7) (a) Boyd, S. A.; Lee, J. F.; Mortland, M. M. *Nature* **1988**, *333*, 345. (b) Jaynes, W. F.; Boyd, S. A. *Clays Clay Miner.* **1991**, *39*, 428. (c) Xu, S.; Boyd, S. A. *Environ. Sci. Technol.* **1995**, *29*, 3022.

(8) Theng, B. K. G. *The Chemistry of Clay Organic Reactions*; Wiley-Interscience: New York, 1972.

(9) Chopra, I. In *Mechanisms of Action of Chemical Biocides: Their Study and Exploitation*; Denyer, S. P., Hugo, W. B., Eds.; Blackwell Scientific Publications: Oxford, 1991; p 45.

(10) (a) Barrer, R. M.; Dicks, L. W. R. *J. Chem. Soc. A* **1967**, 1523. (b) Carrado, K. A. *Ind. Eng. Chem.* **1992**, *31*, 1654. (c) Carrado, K. A.; Forman, J. E.; Botto, R. E.; Winans, R. E. *Chem. Mater.* **1993**, *5*, 472. (d) Carrado, K. A.; Winans, R. E.; Botto, R. E. U.S. Patent 5,308,808, 1994. (e) Carrado, K. A.; Thiyagarajan, P.; Elder, D. L. *Clays Clay Miner.* **1996**, *44*, 506.

(11) Kresge, C. T.; Leonowicz, M. E.; Roth, W. J.; Vartuli, J. C.; Beck, J. S. *Nature* **1992**, *359*, 710.

(12) Beck, J. S.; Vartuli, J. C.; Roth, W. J.; Leonowicz, M. E.; Kresge, C. T.; Schmitt, K. D.; Chu, C. T.-W.; Olson, D. H.; Sheppard, E. W.; McCullen, S. B.; Higgins, J. B.; Schlenker, J. L. *J. Am. Chem. Soc.* **1992**, *114*, 10834.

(13) Mann, S. *Nature* **1993**, *365*, 499.

(14) Mann, S.; Archibald, D. D.; Didymus, J. M.; Douglas, T.; Heywood, B. R.; Meldrum, F. C.; Reeves, N. J. *Science* **1993**, *261*, 1286.

(15) Monnier, A.; Schuth, F.; Huo, Q.; Kumar, D.; Margolese, D. I.; Maxwell, R. S.; Stucky, G. D.; Krishnamurty, M.; Petroff, P. M.; Firouzi, A.; Janicke, M.; Chmelka, B. F. *Science* **1993**, *261*, 1299.

(16) Huo, Q.; Margolese, D. I.; Ciesla, U.; Feng, P.; Gier, T. E.; Sieger, P.; Leon, R.; Petroff, P. M.; Schuth, F.; Stucky, G. D. *Nature* **1994**, *368*, 317.

(17) Huo, Q.; Margolese, D. I.; Ciesla, U.; Demuth, D. G.; Feng, P.; Gier, T. E.; Sieger, P.; Firouzi, A.; Chmelka, B. F.; Schuth, F.; Stucky, G. D. *Chem. Mater.* **1994**, *6*, 1176.

(18) Fyfe, C. A.; Fu, G. *J. Am. Chem. Soc.* **1995**, *117*, 9709.

(19) Chen, C. Y.; Li, H. X.; Davis, M. E. *Micropor. Mater.* **1993**, *2*, 17.

(20) Chen, C. Y.; Burkett, S. L.; Li, H. X., Davis, M. E. *Micropor. Mater.* **1993**, *2*, 27.

(21) Stucky, G. D.; Monnier, A.; Schuth, F.; Huo, Q.; Kumar, D.; Margolese, D. I.; Krishnamurty, M.; Petroff, P. M.; Firouzi, A.; Janicke, M.; Chmelka, B. F. *Mol. Cryst. Liq. Cryst.* **1994**, *240*, 187.

(22) Vartuli, J. C.; Schmitt, K. D.; Kresge, C. T.; Roth, W. J.; Leonowicz, M. E.; McCullen, S. B.; Hellring, S. D.; Beck, J. S.; Schlenker, J. L.; Olson, D. H.; Sheppard, E. W. *Stud. Surf. Sci. Catal.* **1994**, *84A*, 53.

(23) Behrens, P.; Stucky, G. D. *Angew. Chem., Int. Ed. Engl.* **1993**, *32*, 696.

(24) Branton, P. J.; Hall, P. G.; Sing, K. S. W. *J. Chem. Soc., Chem. Commun.* **1993**, 1257.

(25) Inagaki, S.; Fukushima, Y.; Kuroda, K. *J. Chem. Soc., Chem. Commun.* **1993**, 680.
(26) Akporiaye, D.; Hansen, E. W.; Schmidt, R.; Stocker, M. *J. Phys. Chem.* **1994**, *98*, 1926.
(27) Alfredsson, V.; Keung, M.; Monnier, A.; Stucky, G. D.; Unger, K. K.; Schuth, F. *J. Chem. Soc., Chem. Commun.* **1994**, 921.
(28) Bellusi, G.; Perego, G.; Carati, A.; Peratello, S.; Massara, E. P.; Perego, G. *Stud. Surf. Sci. Catal.* **1994**, *84A*, 85.
(29) Coustel, N.; Di Renzo, F.; Fajula, F. *J. Chem. Soc., Chem. Commun.* **1994**, 967.
(30) Feuston, B. P.; Higgins, J. B. *J. Phys. Chem.* **1994**, *98*, 4459.
(31) Janicke, M.; Kumar, D.; Stucky, G. D.; Chmelka, B. F. *Stud. Surf. Sci. Catal.* **1994**, *84A*, 243.
(32) Schmidt, R.; Akporiaye, D.; Stocker, M.; Ellstad, O. H. *J. Chem. Soc., Chem. Commun.* **1994**, 1493.
(33) Schmidt, R.; Akporiaye, D.; Stocker, M.; Ellstad, O. H. *Stud. Surf. Sci. Catal.* **1994**, *84A*, 61.
(34) Wu, C. G.; Bein, T. *Science* **1994**, *264*, 1757.
(35) Wu, C. G.; Bein, T. *Stud. Surf. Sci. Catal.* **1994**, *84C*, 2269.
(36) Fukushima, Y.; Tani, M. *J. Chem. Soc., Chem. Commun.* **1995**, 241.
(37) (a) Finkelmann, M. A.; Schafheutle, M. A. *Colloid Polym. Sci.* **1986**, *264*, 786. (b) Neumann, R.; Ringsdorf, H. *J. Am. Chem. Soc.* **1986**, *108*, 487. (c) Neumann, R.; Ringsdorf, H.; Patton, E. V.; O'Brien, D. F. *Biochim. Biophys. Acta* **1987**, *898*, 338. (d) Ringsdorf, H.; Schlarb, B.; Venzmer, J. *Angew. Chem., Int. Ed. Engl.* **1988**, *27*, 114.
(38) (a) Li, D. Q.; Ratner, M. A.; Marks, T. J.; Zhang, C.; Yang, J.; Wong, G. K. *J. Am. Chem. Soc.* **1990**, *112*, 7389. (b) Wood, J.; Sharma, R. *Langmuir* **1994**, *10*, 2307.
(39) (a) Katz, H. E.; Scheller, G.; Putvinski, T. M.; Schilling, M. L.; Wilson, W. L.; Chidsey, C. E. D. *Science* **1991**, *254*, 1485. (b) Cao, G.; Hong, H.-G.; Mallouk, T. E. *Acc. Chem. Res.* **1992**, *25*, 420.(c) Vermeulen, L. A.; Thompson, M. E. *Nature* **1992**, *358*, 656. (d) Vermeulen, L. A.; Snover, J.; Sapochak, L. S.; Thompson, M. E. *J. Am. Chem. Soc.* **1993**, *115*, 11767. (e) Snover, J.; Thompson, M. E. *J. Am. Chem. Soc.* **1994**, *116*, 765.
(40) Glasser, R. H.; Wilkes, G.; Bronnimann, C. E. *J. Non-Cryst. Solids* **1989**, *113*, 73.
(41) Schaefer, D. W.; Keefer, K. D. *Mater. Res. Soc. Symp. Proc.* **73**, 277.
(42) Plueddemann, E. P. *Silane Coupling Agents*; Plenum Press: New York, 1982; Chapter 3.
(43) (a) Borisov, S. N.; Voronkov, M. G.; Lukevits, E. Y. *Organosilicon Heteropolymers and Heterocompounds*; Plenum Press: New York, 1970; p 255. (b) Baney, R. H.; Itoh, M.; Sakakibara, A.; Suzuki, T. *Chem. Rev.* **1995**, *95*, 1409.
(44) Dagan, G.; Sampath, S.; Lev, O. *Chem. Mater.* **1995**, *7*, 446.
(45) Plueddemann, E. P. *Silane Coupling Agents*; Plenum Press: New York, 1982; pp 94−97.
(46) (a) Veblen, D. R. In *Electron-Optical Methods in Clay Science;* Mackinnon, I. D. R., Mumpton, F. A., Eds.; The Clay Mineral Society: Boulder, CO, 1990; pp 35−36. (b) Mackinnon, I. D. R. In *Electron-Optical Methods in Clay Science;* Mackinnon, I. D. R., Mumpton, F. A., Eds.; The Clay Mineral Society: Boulder, CO, 1990; pp. 95−98.
(47) Reynolds, R. C. In *Modern Powder Diffraction*; Bish, D. L., Post, J. E., Eds.; Mineralogical Society of America: Washington, DC, 1989; p 147.
(48) Brown, G.; Brindley, G. W. In *Crystal Structures of Clay Minerals and Their X-ray Identification*; Brindley, G. W., Brown, G., Eds.; Mineralogical Society: London, 1980; Chapter 5.
(49) Lin, Z.; He, M.; Scriven, E.; Davis, H. T.; Snow, S. A. *J. Phys. Chem.* **1993**, *97*, 3571.
(50) Tiddy, G. J. T. *Phys. Rep.* **1980**, *57*, 1.
(51) Kunitake, T. *Angew. Chem., Int. Ed. Engl.* **1992**, *31*, 709.
(52) Moore, D. M.; Reynolds, R. C. *X-Ray Diffraction and the Identification and Analysis of Clay Minerals*, Oxford University Press: New York, 1989, p 86.
(53) Jenkins, R. In *Modern Powder Diffraction*; Bish, D. L.; Post, J. E., Eds., Mineralogical Society of America: Washington, DC, 1989, p 31.
(54) Reynolds, R. C. In *Modern Powder Diffraction*; Bish, D. L., Post, J. E., Eds.; Mineralogical Society of America: Washington, DC, 1989; p 164.
(55) Reference 54, p 174.
(56) Bailey, S. W. In *Crystal Structures of Clay Minerals and Their X-ray Identification*; Brindley, G. W., Brown, G., Eds.; Mineralogical Society: London, 1980; Chapter 1.
(57) IR bands in cm^{-1}: AlnDS 441, 517, 688, 721, 788, 853, 1023, 1178, 1210, 1240, 1268, 1323, 1343, 1378, 1408, 1467, 1641, 2851, 2920, 2957, 3370. AlnOS 420, 470, 688, 721, 785, 852, 1019, 1184, 1212, 1232, 1342, 1378, 1409, 1466, 1641, 2853, 2923, 2958, 3340. AlnPS 475, 550, 838, 1011, 1193, 1223, 1271, 1304, 1338, 1377, 1402, 1461, 1636, 2874, 2926, 2959, 3380. AlMPS 422, 478, 601, 656, 701, 817, 940, 978, 1012, 1067, 1170, 1298, 1324, 1405, 1454, 1574, 1635, 1717, 2922, 2955, 3108, 3420, 3487. AliBS 472, 593, 667, 734, 837, 1040, 1227, 1331, 1366, 1382, 1402, 1467, 1634, 2625, 2871, 2954, 3403. AlPhS 489, 536, 700, 742, 848, 998, 1027, 1061, 1131, 1429, 1489, 1593, 1630, 3050, 3071, 3385, 3569. MgnDS 482, 576, 689, 721, 787, 957, 1083, 1104, 1294, 1378, 1390, 1409, 1466, 2782, 2853, 2924, 2956, 3728. MgnOS 414, 445, 463, 543, 688, 722, 778, 834, 858, 1027, 1112, 1183, 1213, 1232, 1379, 1410, 1466, 2854, 2924, 2956, 3679, 3701, 3725. MgMPS 478, 536, 654, 696, 771, 816, 847, 904, 940, 984, 1012, 1039, 1128, 1167, 1297, 1322, 1405, 1454, 1637, 1718, 2893, 2930, 2955, 3104, 3477, 3690. MgiBS 477, 741, 836, 1095, 1228, 1332, 1366, 1383, 1402, 1466, 1643, 2626, 2720, 2789, 2870, 2954, 3347, 3729. MgPhS 497, 698, 740, 854, 999, 1029, 1133, 1265, 1430, 1490, 1594, 1775, 1822, 1890, 1960, 2850, 2923, 3017, 3051, 3073, 3376, 3621, 3691.
(58) Andrianov, K. A.; Izmaylov, B. A. *J. Organomet. Chem.* **1967**, *8*, 435.
(59) Silverstein, R. M.; Bassler, G. C.; Morrill, T. C. *Spectrometric Identification of Organic Compounds*; Wiley: New York, 1991; p 104.
(60) (a) Ukrainczyk, L.; Bellman, R. A.; Smith, K. A.; Boyd, J. E. *Mater. Res. Soc. Symp. Proc.*, in press. (b) Smith, K. A.; Boyd, J. E.; Ukrainczyk, L.; Bellman, R. A. To be submitted.
(61) Zeigler, R. C.; Maciel, G. E. *J. Phys. Chem.* **1991**, *95*, 7345.
(62) (a) Fatunmbi, H. O.; Bruch, M. D.; Wirth, M. J. *Anal. Chem.* **1993**, *65*, 2048. (b) Wirth, M. J.; Fatunmbi, H. O. *Anal. Chem.* **1993**, *65*, 822.
(63) Engelhardt, G.; Michel, D. *High-Resolution Solid-State NMR of Silicates and Zeolites*; Wiley: New York, 1987; p 424.
(64) (a) Williams, E. A. *Annu. Rep. NMR Spectrosc.* **1983**, *15*, 235. (b) Williams, E. A.; Cargioli, J. D. *Annu. Rep. NMR Spectrosc.* **1979**, *9*, 287.
(65) (a) Sindorf, D. W.; Maciel, G. E. *J. Am. Chem. Soc.* **1983**, *105*, 3767. (b) Bein, T.; Carver, R. F.; Farlee, R. D.; Stucky, G. D. *J. Am. Chem. Soc.* **1988**, *110*, 4546. (c) Ringsdorf, H.; Schlarb, B.; Venzmer, J. *Angew. Chem., Int. Ed. Engl.* **1988**, *27*, 114. (d) Schlotten, A. B.; de Haan, J. W.; Claessens, H. A.; van de Ven, L. J. M.; Cramers, C. A. *Anal. Chem.* **1994**, *66*, 4085.
(66) Engelhardt, D.; Michel, D. *High-Resolution Solid-State NMR of Silicates and Zeolites*; Wiley: New York, 1987; p 179.
(67) Israelachvili, J. N.; Mitchell, D. J.; Ninham, B. W. *J. Chem. Soc. Faraday Trans. 2* **1976**, *72*, 1526.
(68) Mizutani, T.; Fukushima, Y.; Okada, A.; Kamigaito, O. *Bull. Chem. Soc. Jpn.* **1990**, *63*, 2094.
(69) Mehring, M. *High Resolution NMR Spectroscopy of Solids*, 2nd ed.; Springer-Verlag: New York, 1983.
(70) Bish, D. L.; Duffy, C. J. In *Thermal Analysis in Clay Science;* Stucki, J. W., Bish, D. L.; Mumpton, F. A., Eds.; The Clay Mineral Society: Boulder, CO, 1990; p 124.
(71) Grimshaw, R. W. *The Chemistry and Physics of Clays and Other Ceramic Materials*, 4th ed.; Wiley-Interscience: New York, 1971; pp 701−721.
(72) (a) Seddon, J. M.; Templer, R. H. *Philos. Trans. R. Soc. London A* **1993**, *344*, 377. (b) Mariani, P.; Luzzati, V.; Delacroix, H. *J. Mol. Biol.* **1988**, *204*, 165.
(73) Chapman, D.; Williams, R. M.; Ladbrooke, B. D. *Chem. Phys. Lipids* **1967**, *1*, 445.
(74) Luzzati, V. In *Biological Membranes;* Chapman, D., Ed.; Academic Press: London, 1968; pp 98−99.
(75) Larson, K.; Al-Mamun, M. A. *Chem. Phys. Lipids* **1974**, *12*, 176.